JOURNAL OF MATERIALS SCIENCE 7 (1972) 316–324

A Metallographic Study of Superplasticity in a Micrograin Aluminium Bronze

G. L. DUNLOP*, D. M. R. TAPLIN†
Department of Mechanical Engineering, University of Waterloo, Waterloo, Ontario, Canada

The microstructures of micrograin Cu-9 to 10% Al-0 to 4% Fe alloys, which are superplastic at 800°C, have been determined. Metallographic studies after deformation at 800°C over a range of strain-rates encompassing the three stage strain-rate hardening behaviour common to superplastic materials show that in the low strain-rate range, below that for high values of the strain-rate sensitivity exponent (m), clumps of grains slide together as units with considerable flow in the matrix close to sliding interfaces. After deformation in this low strain-rate range there is no evidence for dislocation motion within the grains. With increasing strain-rate, through and beyond the strain-rate range where peak values of m are recorded, evidence for dislocation motion steadily increases; the tendency for clumps of grains to slide together diminishes; and there is decreased flow in the matrix about the sliding interfaces. The strain-rate for maximum m shows a strong dependence on the proportion of β phase in the microstructure and the presence of iron which acts to refine the grain size. These observations are explained in terms of a flow mechanism whereby the high strain-rate sensitivity range occurs intermediate between a low strain-rate range, where sliding is accommodated by diffusion, and a high strain-rate range, where accommodation is by dislocation movement through the matrix.

1. Introduction

The phenomenology of superplasticity and the several mechanisms which have been proposed to explain the behaviour have been described in two recent reviews [1, 2]. The most important phenomenological feature of micrograin superplasticity is the nature of the variation of flow stress with strain-rate. Superplastic flow occurs over an intermediate strain-rate range within which the flow stress is highly strain-rate sensitive. At strain-rates faster or slower than this range decreasing values of the strain-rate sensitivity exponent, m, are recorded. It is clear that the nature of the flow mechanism must change with strain-rate to produce this behaviour. This paper describes the microstructure of a superplastic micrograin aluminium bronze and some of the metallographic differences which have been detected after straining at 800°C over a range of strain-rates spanning the three-stage behaviour just described. The effect of varying the alloying content in the range 9 to 10% Al and 0 to 4% Fe on the flow stress strain-rate relation is also examined. These observations are then explained in terms of a likely mechanism for micrograin superplasticity. The major alloy which was used (CDA Alloy 619), has a nominal composition of Cu-9.5% Al-4% Fe, and was developed by Olin Corporation as an oxidation resistant alloy possessing high strength at ambient temperatures [3]. The detailed superplastic tensile behaviour of this alloy has been described elsewhere [4].

2. Experimental Procedure

Alloys of the composition shown in table I were received in the form of 1 mm thick cold rolled sheet from which tensile specimens with tensile axes parallel to the rolling direction were cut and strained in air at 800°C. Change-rate tests to determine m over a wide range of strain-rates were carried out on all four alloys according to

*Formerly Graduate Student, Department of Mechanical Engineering, University of Waterloo, Ontario, Canada. Present address: Department of Metallurgy, University of Cambridge, England.
†Associate Professor, Department of Mechanical Engineering, University of Waterloo, Waterloo, Ontario, Canada.

the procedure of Backofen [5]. To minimise the effect of errors inherent in this method [4] and enable direct comparisons to be made, each test was conducted in identical fashion so that each corresponding change in cross-head speed occurred at the same elongation for each alloy. Elevated temperature tensile tests at various nominal strain-rates were performed on alloy 619. To preserve the high temperature microstructure after straining, specimens were rapidly cooled from the test temperature with an iced water spray. For interrupted tests the cross-head motion was stopped and the bottom loading pin released before quenching. Specimens which had been annealed at 800°C followed by a water quench and samples cut from the gauge length of strained tensile specimens were examined metallographically. Specimens for optical metallography were mechanically polished with a final polish of either a 15 min "skid" polish on a paste of MgO in a 1.5% aqueous ammonium persulphate solution or a 3 min vibratory polish with a similar polishing medium. When required the specimens were electrolytically etched in a 1% chromic acid solution at a potential of about 6 V.

TABLE I Composition of aluminium bronze alloys.

Alloy	% Cu	% Al	% Fe
22	85.9	10.1	4.0
619	86.5	9.5	4.0
23	87.0	8.9	4.1
24	90.5	9.5	—

Thin foils for transmission electron microscopy were prepared by two methods. One method involved punching discs 3 mm in diameter from material which had been ground to approximately 250 μm thickness and then jet polishing the discs, with an apparatus incorporating a PTFE holder, at a potential of 8V in a 33% nitric acid, 67% methanol electrolyte maintained at a temperature below 10°C. In the other method, square specimens of 3.2 mm edge length were cut out with a water cooled SiC cut-off wheel, jet profiled with 20% nitric acid with a current of 2 A, and finally polished at a potential of 6 V in 33% nitric acid, 67% methanol cooled to about −20°C.

The surfaces of deformed specimens were examined for grain boundary sliding offsets in a "Stereoscan" scanning electron microscope. Prior to high temperature testing, these tensile specimens were electropolished, scratched parallel and transverse to the tensile axis with 0.3 μm alumina polishing powder to provide surface fiducial lines, and coated with "Berkatekt" compound to reduce oxidation. Improved resolution in the scanning electron microscope was obtained by vacuum coating the lightly oxidised surfaces with a thin film of gold.

3. Results

The microstructure of cold rolled alloy 619 in the "as-received" condition is shown in fig. 1 and after annealing at 800°C for 30 min in fig. 2. The alloy recrystallises at 800°C to a duplex structure containing approximately equal amounts of α and β phases as predicted by the phase diagram [6]. The phase with light contrast in fig. 2 is the α, Cu-rich fcc solid solution, while the other major phase with dark contrast is the low temperature martensitic transformation product [7, 8] of the elevated temperature β-phase. The rounded particles in fig. 2 were identified by selected area electron diffraction as having a bcc structure with lattice parameter of 2.9Å which is consistent with the iron-rich δ-phase (81.5% Fe, 13.5% Al, 5% Cu) found previously in Cu-Al-Fe alloys [9]. Electron microscopy showed that δ particles often pinned grain boundaries thus restricting grain boundary migration and grain growth.

A dispersion of much finer particles, which were of sub-micron size and cuboid shape, was found by electron microscopy to be dispersed in the martensite and also in that region of the α-phase close to the α/martensite interface (fig. 3). Strain contrast effects were evident about the particles in the martensite but not about those in the α-phase. Selected area diffraction

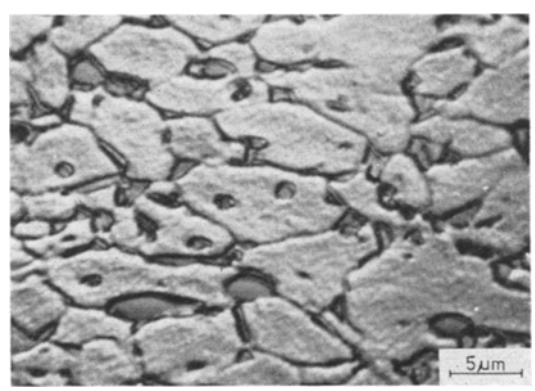

Figure 1 Microstructure of cold rolled alloy 619 sheet in the as-received condition.

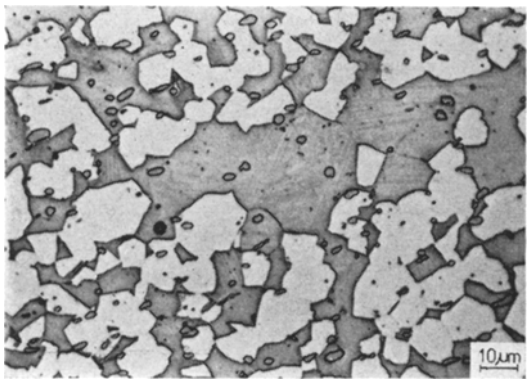

Figure 2 Alloy 619 annealed at 800° C for 30 min followed by a water quench.

showed these particles to have a lattice parameter of 2.9Å consistent with the δ-phase mentioned above. Subsequent dark field imaging showed a strong orientation relation between individual particles and this, together with an observation of coarsening upon annealing for prolonged periods at 800° C suggests that the particles are present in the β-phase at 800° C. It is apparent that the submicron particles present in the α-phase close to the α/martensite interface were left behind after movement of the α/β interface in the direction of the β-phase, on initial cooling during the quench from 800° C, due to the increase of the equilibrium amount of α with decreasing temperature [6].

Alloys 22, 23 and 24 recrystallised in a similar fashion to alloy 619 except that alloy 24, which contained no iron, had no δ-phase present and the microstructure of this alloy was significantly more coarse. As expected from operation of the lever rule in the phase diagram [6] the relative amounts of α- and β-phases varied with aluminium content. Measurements of the relative amounts of α- and β-phases after annealing cold rolled material for various times at 800° C and water quenching indicated that recrystallisation was complete within 30 min of reaching that temperature. Results of random linear intercept measurements of the metallographic mean free path, L, in α- and β- phases and the relative volumes of either phase after annealing for 30 min at 800° C and water quenching are presented in table II. Boundaries between grains of the same phase were not easily revealed by etching but from the distribution of nodal points in optical micrographs the average grain diameter in both α- and β-phases of the iron-containing alloys was estimated to be approximately 8 μm after 30 min at 800° C. The grain size of alloy 24, which contained no iron, was estimated to be 15 to 20 μm after a similar treatment.

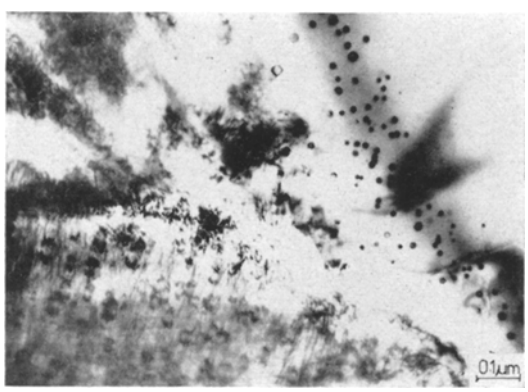

Figure 3 Sub-micron δ particles in martensite and also present in the α-phase close to the α/martensite interface.

TABLE II Effect of alloying content on phase size and relative amounts of α- and β-phases.

Alloy	Lα (μm)	Lβ (μm)	%α	%β
22, 10.1% Al, 4% Fe	10	16	37	63
619, 9.5% Al, 4% Fe	11.6	14.5	45	55
23, 8.9% Al, 4% Fe	24	7	70	30
24, 9.5% Al, 0% Fe	25	22	51	49

Change-rate tests to determine m over a range of strain-rates at 800° C revealed that there is a marked effect of both Fe and Al content upon the strain-rate at which m is a maximum (fig. 4). When no iron is present, peak values of m occur at very low strain-rates while for alloys containing iron the peak in m occurred at increased strain-rates as the aluminium content was increased. The detailed tensile behaviour of alloy 619 is described elsewhere [4] but the three-stage dependence of flow stress upon strain-rate is reproduced in fig. 5. The microstructural changes which occur during deformation at various strain-rates are considered in relation to this three-stage behaviour.

Optical examination of deformed specimens of alloy 619 revealed that coarsening of both α- and β-phases took place during deformation and that this coarsening increased with both the amount of strain and the duration of the test so that maximum coarsening occurred when specimens were deformed to high strains at low strain-rates. The amount of coarsening was always small, however, in comparison to that observed by

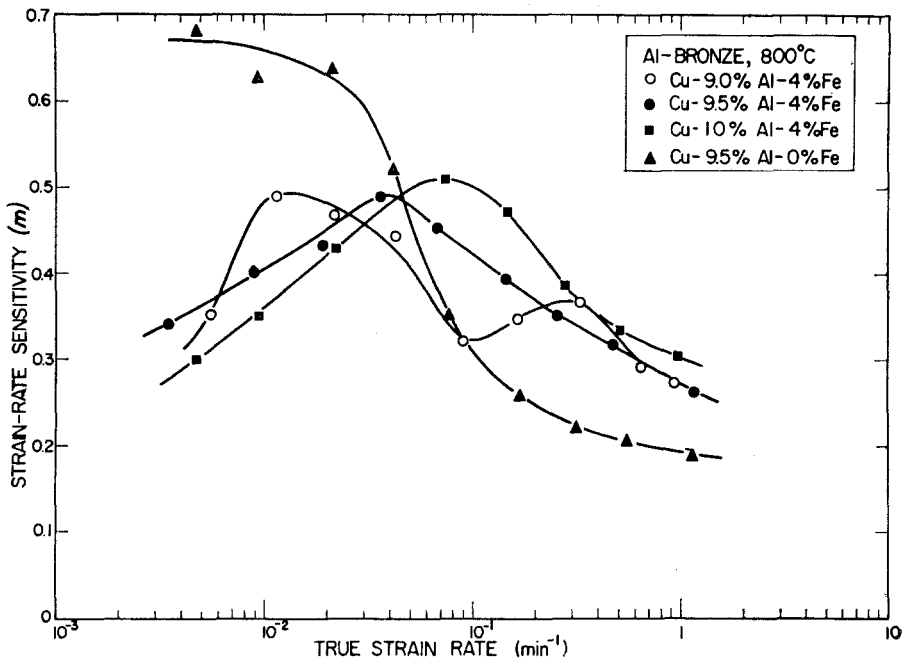

Figure 4 The effect of alloying content on the m-$\dot{\epsilon}$ curve.

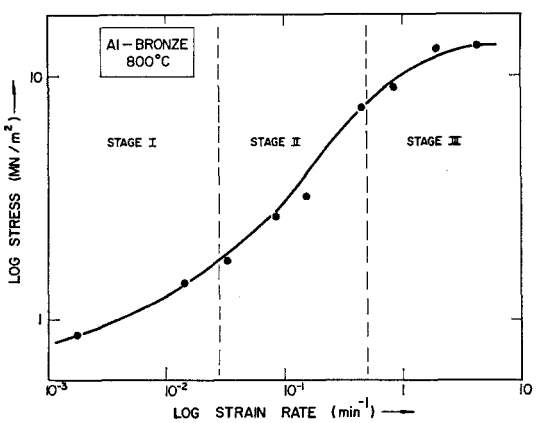

Figure 5 Three stage flow stress/strain-rate behaviour of alloy 619 at 800° C.

Watts and Stowell [10] in the Al-Cu eutectic. Cavities were also observed to form and grow at α/β interfaces and triple junctions when specimens were deformed at strain-rates greater than 7.9×10^{-2} min^{-1} [11].

Specimens of alloy 619 strained at various engineering strain-rates to strains in the range 100 to 550% were examined by transmission electron microscopy. Because the β-phase transformed martensitically on rapid cooling, dislocation structures due to the high temperature deformation were visible only in the α-phase. A range of dislocation configurations associated with different strain-rates was observed and these configurations are summarised in fig. 6. In specimens deformed up to 550% elongation at initial strain-rates below 4×10^{-1} min^{-1} dislocation configurations in many α grains were similar to that of material annealed at 800° C, with an apparent absence of any stable defect structure resulting from the high temperature deformation. However, some grains in specimens deformed at initial strain rates between 10^{-2} min^{-1} and 4×10^{-1} min^{-1} contained arrays of extended partial dislocations on several slip systems (fig. 6a). Similar arrays were not seen in annealed and quenched material or in material deformed at other strain-rates; accordingly it is deduced that they result from high temperature deformation at these strain-rates.

After deformation at the higher initial strain-rate of 7.9×10^{-1} min^{-1} the separation of partial dislocations was considerably less, and tangles of dislocations were often observed (fig. 6b). At the maximum initial strain-rate of 3.9 min^{-1} dislocation tangles were more frequent and subgrains formed in some grains (fig. 6c).

Surfaces of specimens strained to 56%

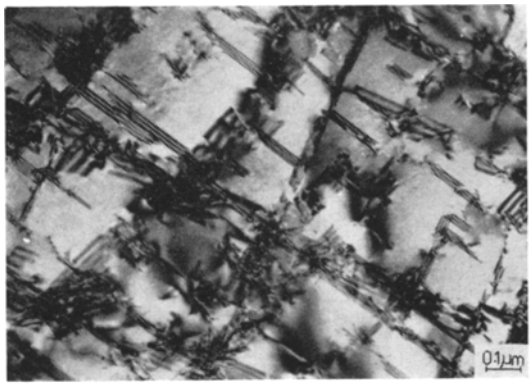

(a)

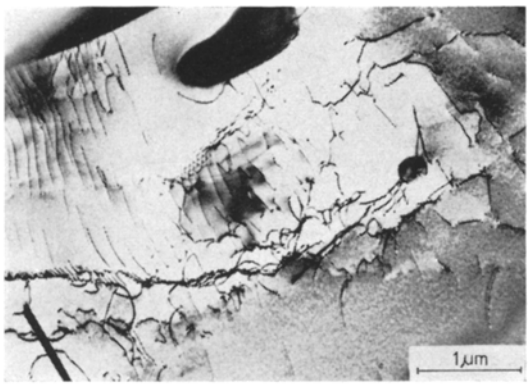

(b)

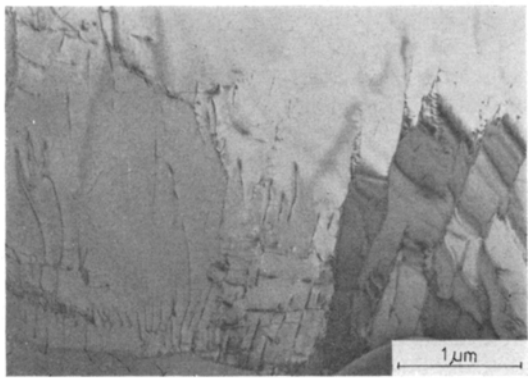

(c)

Figure 6 Dislocation configurations after deformation at 800°C followed by rapid cooling: (a) strain rate 3.9×10^{-2} min^{-1}, 96% elongation; (b) strain-rate 7.9×10^{-1} min^{-1}, 300% elongation; (c) strained 350% to fracture at 3.9 min^{-1}

elongation at strain-rates corresponding to each of the three stages of the flow stress/strain-rate relation (fig. 5) were examined by scanning electron microscopy. Despite the presence of a thin oxide layer on the surface, surface steps and offsets of marker lines, due to the relative translation of grains during high temperature deformation, were clearly visible. As shown by fig. 7 there was a transition in the grain boundary sliding behaviour over the three stage strain-rate range.

During deformation at strain-rates in stage I whole clumps of grains tended to move relative to each other with comparatively little movement between grains within each clump (fig. 7a). The surface dimensions of each clump were such that they were much longer transverse to the stress axis than parallel to the stress axis. Surface markers were considerably curved close to interfaces, where sliding had taken place, indicating either that considerable matrix flow took place in this region or that grain boundary migration took place concurrent with sliding. Freshly exposed grain boundary surfaces were heavily grooved with deep gouge markings, indicating that a considerable rearrangement of material close to the sliding interface had taken place.

During deformation in the fast strain-rate range (stage III) the tendency for clumps of grains to move together was reduced (fig. 7e). Many more grains moved relative to each other but the amount of sliding on individual boundaries was diminished. Marker lines were not curved close to boundaries but finished abruptly at surface offsets. Freshly exposed grain boundary surfaces (fig. 7f) were significantly less grooved than at the slow strain-rate indicating a decreased influence of matrix flow or grain boundary migration close to the interface. At strain-rates in stage II where the flow stress is highly strain-rate sensitive the sliding behaviour (figs. 7c and d) was intermediate between that for stages I and III in all the aspects which have been described.

4. Discussion

With the exception of the defect substructure of elongated stacking faults seen in material deformed at strain-rates in the lower range of stage II, the transmission electron microscope observations on deformed alloy 619 are largely in accord with similar studies on other superplastic alloys [12-16] which had been deformed at strain-rates over a similar generic range. The stacking fault substructure is unique to the present study on material where the α-phase has a very low stacking fault energy [17, 18]. Other superplastic alloys have been shown to be free of

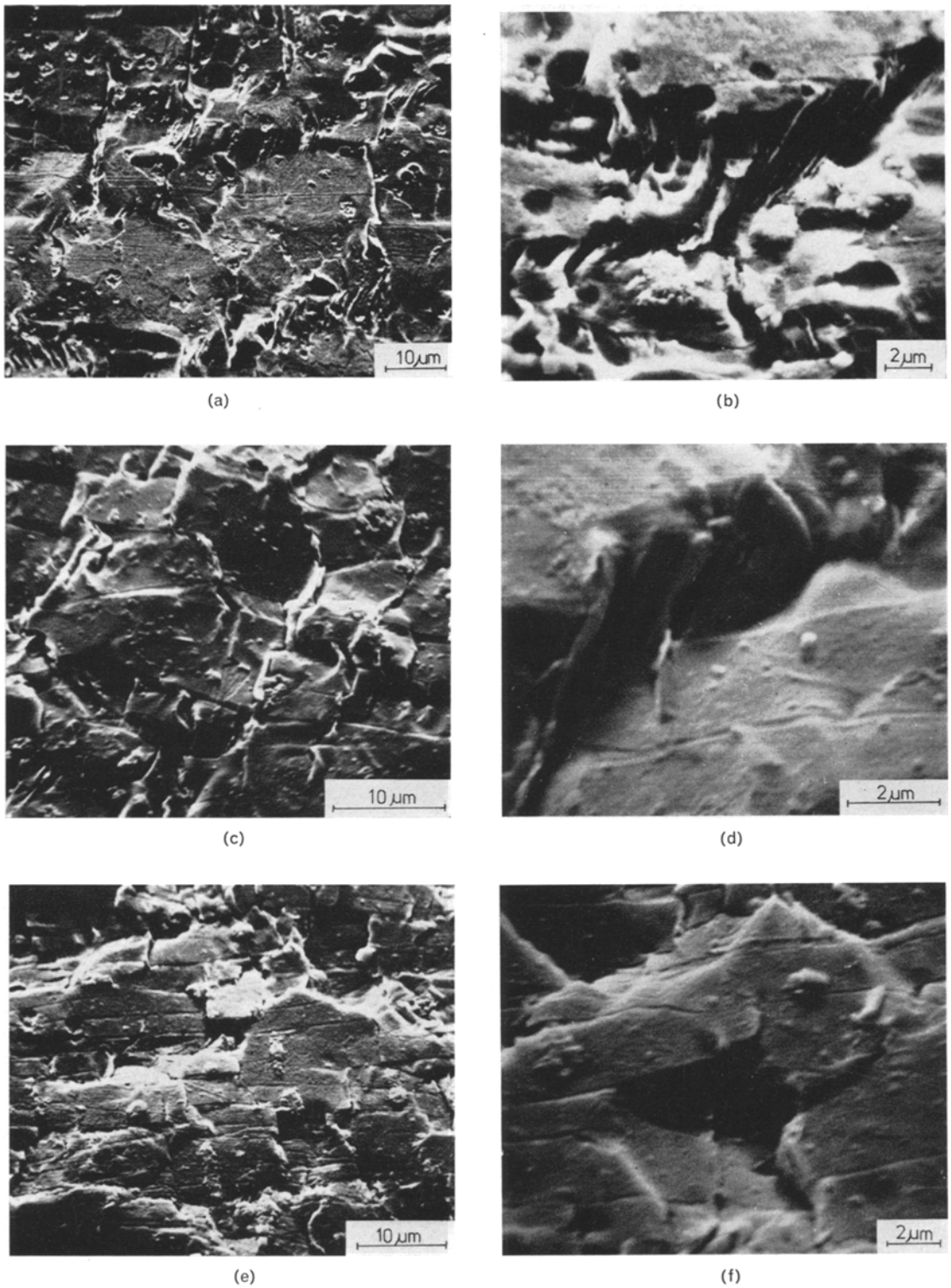

Figure 7 Scanning electron micrographs showing surfaceoffsets, due to grain boundary sliding, after 56% elongation: (a) and (b) strain rate 4.3×10^{-3} min^{-1}; (c) and (d)strain rate 1.05×10^{-1} min^{-1}; (e) and (f) strain rate 4.3 min^{-1}.

defects due to deformation in this range of strain-rates [12-16]. A point to note is that the observed stacking fault separation of partial dislocations (fig. 6a) may be greater at room temperature than at elevated temperatures because the stacking fault energy of Cu-Al solid solutions increases with increasing temperature [18] but this effect could be offset if segregation to stacking faults takes place at elevated temperatures [18]. It is possible, also, that the large areas of stacking fault are partly due to the condensation of vacancies on dissociated dislocations in a manner not dissimilar to the formation of faulted dislocation loops in quenched and aged copper and silver [19]. In the present case the cooling rate from 800°C was not likely to be rapid enough to provide a high supersaturation of vacancies in the matrix at room temperature and so the supersaturation and subsequent condensation of vacancies would have to occur at the testing temperature. The source of vacancies for such a supersaturation could be the sliding grain boundaries. If this is so then it is possible that diffusion creep taking place in association with superplastic deformation, as may be inferred by observation of denuded zones at transverse grain boundaries by Karim [20], may be a secondary process which is not rate controlling but which arises because of an excess vacancy concentration at certain segments of sliding grain boundaries. It should also be noted that such denuded zones are not unequivocally formed by diffusion creep but may arise from grain boundary migration [21].

As concluded by other workers [12, 14, 16] the transition between low and high strain-rate behaviour is associated with an increased resistance to dislocation movement within the α-phase because of an increased number of dislocation interactions. This may be either due to an increase in the number of mobile dislocations with increasing strain-rate or due to a decrease in the ability of time-dependent recovery processes to cope with increased strain-rates. Both effects are likely to occur but, as discussed later, the former is considered to account for the rising flow stress occurring with increased strain-rates in stage II.

The transition from low to high strain-rate behaviour also appears to be accompanied by a transition in the nature of flow about sliding interfaces as shown by the decreased gouging of new surfaces and the decrease in the distortion at grain boundaries of surface fiducial lines as the strain-rate was increased. The heavily gouged nature of surfaces exposed due to grain boundary sliding at interfaces, whose surface intersections were largely transverse to the tensile axis, is associated with the striations observed at transverse grain boundaries after deformation of some other superplastic alloys at similar generic strain-rates within stages I and II [13, 22-25]. When observed in the optical microscope, where relief effects do not appear in such high contrast as under optimum conditions in the scanning electron microscope, these gouged surfaces appeared as striated bands at transverse grain boundaries. The appearance of these surface regions is dependent on the angle of observation in the scanning microscope or the shadowing direction for surface replica studies. In the present instance both the plane of the specimen and the tensile axis were situated at 45° to the electron beam and collector while inspection of the scaning micrographs presented by Lee [13] suggests that his specimen plane was similarly situated except that the tensile axis was at 90° to both incident beam and collector. Under these conditions the striated regions would appear as though they lie largely in the specimen plane. Similarly, the shadowing direction used by Backofen *et al* [22-24] in their replica studies was such that the striated regions appeared to be in the plane of the specimen while the shadowing angle used by Alden [25] shows clearly that the striations lie on surfaces exposed by grain boundary sliding.

An important fact to emerge from the above discussion is that measurements of the elongation of surface grains on the basis of the width of striated bands [13, 22, 23] are based on false premises. Also, evidence cited for elongation of grains only 3 to 4 μm below the surface [22, 23] is negated because in that work the surface grains were removed by electropolishing and surface relief effects would be largely maintained on the new surface for examination. This argument is reinforced by the work of Zehr and Backofen [24] where it was found that surface grain elongation, as estimated from the width of striated bands, did not correspond to the specimen interior where grains were found to show no elongation.

Because striated surfaces appear chiefly at transverse grain boundaries it may be concluded that at strain-rates in stage I a large proportion of the strain due to grain boundary sliding occurs at these grain boundaries while at strain-rates in

stage II a lesser proportion occurs at these boundaries. Also, a large component of the relative translation between sliding grains must occur in a direction perpendicular to the stress axis to produce the large surface offsets. These factors, together with the observation that groups of grains, with the largest surface dimension of the group lying perpendicular to the stress axis, tend to slide together as units and that striated bands were often continuous for several grain widths (see also micrographs in references [13, 22, 23] suggest that at strain-rates in stage I there is a tendency for shear, due to grain boundary sliding, to occur on surfaces of easy glide which bound a number of grains. As suggested by measurements of the dependence of grain boundary sliding on the resolved shear stress on grain boundaries [26] such surfaces would lie across the tensile specimen largely at an angle of 45° to the tensile axis and would behave similarly to a slip plane in a single crystal under tension. There is a certain component of random movement of grains superimposed upon this general bulk movement and this random component apparently increases with increasing strain-rate.

Of the mechanisms proposed for superplastic flow [1, 2] only three purport to explain all three stages of the flow stress/strain-rate relation of fig. 6. These are: the diffusional creep model of Backofen [22-24]; the dynamic recrystallisation model put forward by Packer *et al* [27]; and the grain boundary sliding model proposed by Hart [28] and elaborated upon by Lee [13]. No clear experimental evidence has been provided in support of the dynamic recrystallisation theory and no indication of such a process taking place was noted during *in situ* deformation experiments in the scanning electron microscope [29]. As discussed earlier in this paper much of the metallographic evidence cited in support of the diffusion creep model must be discounted and on a theoretical argument the model is also found to be lacking: a Bingham, or zero strain-rate flow stress associated with grain boundary sliding has been invoked to account for the low values of m at stage I strain-rates [22-24] but Hart [30] has argued that, if the conditions for diffusion creep were operative, grain boundary sliding would also proceed by a similar mechanism and so could not be the rate-limiting process in stage I.

The grain boundary sliding model [28, 13] provides the most satisfactory model for superplastic flow and satisfactorily explains the present observations. In this theory it is considered that the process of grain boundary sliding occurs relatively easily over a wide range of strain-rates but the rate of sliding is limited by plastic flow within grains to relieve stress concentrations which arise at irregularities in the sliding boundary. During deformation in stage I, plastic flow about irregularities in the sliding boundary is by diffusional processes while in stage III, plastic flow in grains is by dislocation movement. Stage II is a transition region between the low and high strain-rate situations, where the flow stress is very sensitive to small changes in strain-rate because of the difference in flow stress between stages I and III. The lower strain-rate bound for stage II occurs when the rate of sliding on some grain boundaries becomes too great for it to be accommodated by diffusional flow, and the stress rises because of the higher stress necessary for dislocation movement. The upper strain-rate bound for stage II occurs when the rate-limiting process in all parts of the polycrystal is matrix flow by dislocation movement.

Measurements made by Lee [13] have suggested that the contribution of grain boundary sliding to overall strain, γ_{gb}, is a maximum at strain-rates within stage II but the techniques used are open to criticism [31]. Also, the change in the nature of intergranular flow over strain-rates in stage II may cause an overestimate of the amount of grain boundary sliding occurring at these and higher strain-rates in comparison to the amount occurring at stage I rates if measurements are made on transverse markers. On the basis of the present observations and micrographs in the literature [13, 20, 22, 23] a more likely relationship between γ_{gb} and strain-rate is that γ_{gb} is high during stage I and decreases with increasing strain-rate through stages II and III. This transition in the amount of grain boundary sliding taking place would be caused by the increased difficulty of accommodation of stress concentrations at the sliding interfaces as indicated by the decreased amount of flow occurring within the matrix about the sliding interfaces and the formation of intergranular cavities at strain-rates greater than the mid-point of stage II in Alloy 619 [11].

Increasing the aluminium content of the iron-containing alloys resulted in stage II of the flow stress/strain-rate behaviour occurring at increased strain-rates. Although detailed grain size (as opposed to phase size) measurements were not made, optical metallography revealed that the

grain size in both phases was similar in all three alloys. It is concluded, therefore, that this effect is a result of the increased proportion of β-phase (and decreased proportion of α-phase) in the microstructure. Postponement of stage II, which arises because of the lack of diffusional accommodation at sliding interfaces, to higher strain-rates as the aluminium content is increased then suggests that either bulk diffusion in the α-phase or diffusion along α/α grain boundaries, rather than β-phase diffusion, may be the diffusion process which is rate limiting in stage I. At a fixed applied strain-rate and with decreasing α-phase content, the rate of sliding at interfaces involving α grains can decrease with proportionally more of the strain being taken up at sliding β/β interfaces so allowing postponement of stage II to higher strain-rates.

For alloy 24, containing no iron, it is likely that the occurrence of stage II at a much lower strain-rate range than for the similar alloy containing 4% Fe (alloy 619) is a result of the grain size effect observed by many other workers [1, 2]. If a large proportion of the strain at a certain imposed strain-rate is to occur by grain boundary sliding, the rate of sliding at individual interfaces of the larger grain size material must be greater than for the material of finer grain size because of the difference in the amount of grain boundary area per unit volume. The onset of stage II must then occur at a much lower applied strain-rate for the material of coarser microstructure.

Acknowledgements

This work has been supported by the National Research Council and Defence Research Board of Canada together with Olin Corporation, Metals Research Laboratory, New Haven, USA. Assistance with electron microscopy from M. H. Lewis and discussions with J. Crane, E. Shapiro, and J. W. Edington are gratefully acknowledged.

References

1. R. H. JOHNSON, *Metall. Rev.* **15** (1970) 145.
2. G. J. DAVIES, J. W. EDINGTON, C. P. CUTLER, and K. A. PADMANABHAN, *J. Mater. Sci.* **5** (1970) 1091.
3. J. CRANE, ASM Conference, Philadelphia, 1969.
4. G. L. DUNLOP and D. M. R. TAPLIN, *J. Mater. Sci.* **7** (1972) 84.
5. W. A. BACKOFEN, I. R. TURNER, and D. M. AVERY, *Trans. ASM* **57** (1964) 980.
6. P. J. MACKEN and A. A. SMITH, "The Aluminium Bronzes" (Copper Development Association, London) 1966.
7. H. SATO, R. S. TOTH, and G. HONJO, *Acta Metallurgica* **15** (1967) 1381.
8. J. R. MOON and R. D. GARWOOD, *J. Inst. Metals* **96** (1968) 17.
9. J. A. MULLENDORE and D. J. MACK, *TMS AIME* **212** (1958) 252.
10. B. M. WATTS and M. J. STOWELL, *J. Mater. Sci.* **6** (1971) 228.
11. J. CRANE, G. L. DUNLOP, E. SHAPIRO, and D. M. R. TAPLIN. To be published.
12. A. BALL and M. M. HUTCHINSON, *Met. Sci. J.* **3** (1969) 1.
13. D. LEE, *Acta Metallurgica* **17** (1969) 1057.
14. H. W. HAYDEN and J. H. BROPHY, *Trans. ASM* **61** (1968) 542.
15. H. W. HAYDEN, R. C. GIBSON, H. F. MERRICK, and J. H. BROPHY, *ibid* **60** (1967) 3.
16. E. H. LEE and E. E. UNDERWOOD, *Met. Trans.* **1** (1970) 1399.
17. A. HOWIE and P. R. SWANN, *Phil. Mag.* **6** (1961) 1215.
18. P. C. J. GALLAGHER, *Met. Trans.* **1** (1970) 2429.
19. L. M. CLAREBOROUGH, *Phil. Mag.* **13** (1966) 285.
20. A. KARIM, D. L. HOLT, and W. A. BACKOFEN, *TMS AIME* **245** (1969) 1131.
21. D. LEE, *Scripta Met.* **3** (1969) 893.
22. W. A. BACKOFEN, F. J. AZZARTO, G. S. MURTY, and S. W. ZEHR, "Ductility", *ASM* (1968) 279.
23. W. A. BACKOFEN, G. S. MURTY, and S. W. ZEHR, *TMS AIME* **242** (1968) 329.
24. S. W. ZEHR and W. A. BACKOFEN, *Trans. ASM* **61** (1968) 300.
25. T. H. ALDEN, *Acta Metallurgica* **15** (1967) 469.
26. R. C. GIFKINS, A. GITTINS, R. L. BELL, and T. G. LANGDON, *J. Mater. Sci.* **3** (1968) 306.
27. C. M. PACKER, R. H. JOHNSON, and O. D. SHERBY, *TMS AIME* **242** (1968) 2485.
28. E. W. HART, *Acta Metallurgica* **15** (1967) 1545.
29. D. J. DINGLEY, Scanning Electron Microscopy 1970, (IIT Research Institute, Chicago, 1970) 329.
30. E. W. HART, *G.E. Research Report* (1969) No. 69-C-029.
31. T. G. LANGDON and R. C. GIFKINS, *Scripta Met.* **4** (1970) 337.

Received 23 September and accepted 8 October 1971.